

High resolution photodetachment study of OH⁻ and OD⁻ in the threshold region 7000–6450 Å*

H. Hotop[†] and T. A. Patterson

Joint Institute for Laboratory Astrophysics, University of Colorado, Boulder, Colorado 80302

W. C. Lineberger[‡]

Joint Institute for Laboratory Astrophysics, and Department of Chemistry, University of Colorado, Boulder, Colorado 80302

(Received 29 October 1973)

The photodetachment of OH⁻ and OD⁻ ions has been studied in the range 7000–6450 Å, utilizing a tunable, narrow-bandwidth (0.5–1 Å) dye laser as the light source. A detailed comparison of the observed cross section with model calculations is made, yielding the following results:

E.A.(OH) = (14 723 ± 15) cm⁻¹, E.A.(OD) = (14 703 ± 15) cm⁻¹. The observed isotope effect for the electron affinity can be ascribed almost entirely to differences in the position of the ground rotational state in OH(²Π_{3/2}) and OD(²Π_{3/2}); the implications of this result for the vibrational frequency of the negative ions are discussed. The energy dependence of the observed cross section indicates the influence of the electron–permanent dipole moment interaction in the final channel on the threshold behavior, which is found to be sharper than that expected in the absence of such an interaction.

I. INTRODUCTION

Tunable laser light sources, with their inherent advantages of high photon flux and narrow bandwidth, and particularly dye lasers in the range 3500–7000 Å, have recently been used to make a major improvement in photodetachment studies.^{1–4} With these sources we have made the first reliable test of the theoretical threshold law for the photodetachment of atomic negative ions^{1,3,4} providing electron affinities of S,¹ Se,³ and Au⁴ atoms with an accuracy of about 0.5 meV. In addition we have been able to study C₂⁻ negative ions² via two-photon detachment, in which a real intermediate state (an excited bound state of C₂⁻) is populated by absorption of a first photon with a subsequent transition into the continuum by absorption of a second photon. However, to date there has been no high resolution (Δλ ≲ 1 Å) photodetachment threshold study of a molecular negative ion for the purpose of accurately determining its electron affinity.

In this paper we report such a measurement in which OH⁻ and OD⁻ photodetachment is studied in the range 7000–6450 Å. The interpretation of the data is much more complicated than for photodetachment of atomic negative ions because of the manifold of transitions involved and our lack of knowledge of the threshold law and of the internal energy state distribution of the negative ions. Being aware of these problems, we chose a molecular negative ion that has been studied before by Branscomb^{5,6} and Smith⁵ with a resolution of 100 Å in the range 4000–7500 Å, namely the OH⁻(OD⁻) ion. The complexity of the problem is reflected in the analysis which Branscomb⁶ carried out in order to deduce the electron affinity of OH and OD as (1.83 ± 0.04) eV and to determine the internuclear separation and the vibrational frequency of the negative ions. The latter two quantities were found to be equal to those of the neutral molecules within experimental uncertainties. The similarity of the structure of OH(X²Π₁) and OH⁻(¹Σ⁺) had also been predicted by Cade⁷ who carried out a Hartree–Fock calculation for these systems.

More recently, Celotta, Bennett, and Hall⁸ have measured the energy spectrum of electrons detached from OH⁻ ions by an argon-ion laser beam (4880 Å). They confirm Branscomb's findings, and, from their observation that the (1,0) vibrational transition is at least 1600 times weaker than the (0,0) transition, one can conclude that $\nu_e(\text{OH}^-) = \nu_e(\text{OH})$ to within 0.001 Å (0.1%). We shall make use of this result in the interpretation of our data.

II. EXPERIMENTAL

The technique used in the present work has been described in detail.³ Briefly, a 2 keV hydroxyl negative ion beam is created in a hot cathode plasma ion source, mass analyzed and crossed by the light from a flash-lamp-pumped, grating-tuned dye laser (cresyl violet acetate + rhodamine 6 G) with a bandwidth of 0.5–1 Å. When the ion source is operated with a mixture of NH₃ and O₂, ¹⁶OH⁻ ions are produced; if a mixture of D₂ and O₂ is used, ¹⁶OD⁻ ions are produced. In the latter case, the contamination of the ¹⁶OD⁻ beam by ¹⁸O⁻ ions is > 4 × 10⁻⁴ (as estimated from the size of the ¹⁶O⁻ mass peak, using the natural ¹⁶O/¹⁸O isotopic ratio), thereby leading to a negligible contribution to the observed signal in the wavelength region covered. Typical mass analyzed ion currents are 100 nA. Photodetachment events are detected by measuring the amplified secondary electron current ejected by the fast neutral molecules at the cathode of a multiplier. Thus the quantity actually measured is a relative cross section for production of neutrals. Since no photodissociation channels are open in the photon energy range employed, the measured quantity is a relative cross section for photodetachment of OH⁻(OD⁻) ions.

III. MEASUREMENTS

The general shape of the cross section, observed in the range 14275–15475 cm⁻¹ (7000–6450 Å) and shown in Fig. 1, is similar to that measured by Smith and Brans-

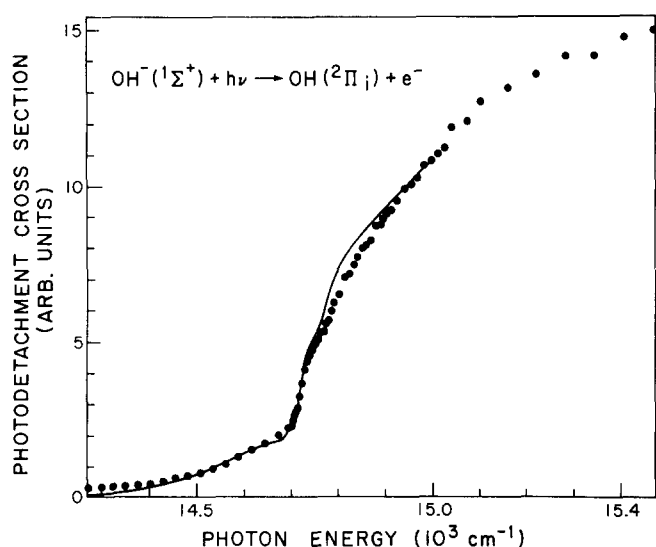


FIG. 1. OH⁻ photodetachment cross section in the energy range 14 300–15 400 cm⁻¹ (7000–6500 Å). The dots represent the experimental data, with the sharp onset near 14 700 cm⁻¹ corresponding to the opening of the Q branches in the ²Π_{3/2} final state. The solid line is a fit to the data using an E^{1/4} threshold law, a negative ion rotational temperature of 1200 °K, and rotational line strengths as discussed in the text.

comb.^{5,6} There is, however, a rather prominent sharp onset for both OH⁻ and OD⁻ detachment at about 14700 cm⁻¹, which could not be detected in the low resolution measurement. The OH⁻ and OD⁻ photodetachment data over the limited range 14675–14775 cm⁻¹ are presented in detail in Fig. 2. The solid lines represent a model fit to these data, and will be discussed in Sec. IV. D.

The rather steep rise observed in Fig. 2, which occurs over a range of 50 cm⁻¹ (≈ 6 meV), is due to the opening of what we shall call the Q-rotational branch (see Sec. IV. B for details) for transitions from OH⁻(OD⁻)¹Σ⁺ to OH(OD)²Π_{3/2}. The major conclusions of this paper will be drawn from a detailed inspection of this part of the observed cross section.

Referring to Fig. 1, there is, in addition to the onset with steepest slope at about 14725 cm⁻¹, an additional rise at slightly higher energy with the steepest slope occurring near 14800 cm⁻¹. This feature is a result of the opening of the Q branch terminating in the OH(²Π_{1/2}) state. As far as the detection of single rotational onsets is concerned, we can say that we have seen some structure in the region below 14700 cm⁻¹, which appears to correspond to P-branch transition channel openings. The signal-to-noise ratio was not good enough, however, to allow us to investigate these structures in detail.

IV. DISCUSSION

A. Energy levels in OH(²Π_i) and OH⁻(¹Σ⁺)

The molecular structure constants for the OH(²Π_i) ground electronic state are well known from spectroscopy.^{9,10} The ones used in the present study for analysis of the data are summarized in Table I. The term energy of the different rotational levels of interest can be written (see Fig. 3)

$$T(\text{OH } X^2\Pi_{3/2}; v'=0; J') = T_e^{\text{OH}} + E_0^{\text{OH}} + F_1^{\text{OH}}(J'), \quad (1a)$$

$$T(\text{OH } X^2\Pi_{1/2}; v'=0; J') = T_e^{\text{OH}} + E_0^{\text{OH}} + F_2^{\text{OH}}(J'), \quad (1b)$$

$$T(\text{OH}^- ^1\Sigma^+; v''=0; J'') = E_0^{\text{OH}^-} + F^{\text{OH}^-}(J''), \quad (1c)$$

where T represents the energy as measured relative to the bottom of the potential well of the negative ions. E_0 is the respective vibrational zero-point energy including the Y_{00} term from the Dunham expansion¹¹

$$E_0 = Y_{00} + \frac{\omega_e}{2} - \frac{\omega_e x_e}{4} + \frac{\omega_e y_e}{8} + \dots, \quad (2)$$

$$Y_{00} = \frac{B_e}{4} + \frac{\alpha_e \omega_e}{12 B_e} + \frac{\alpha_e^2 \omega_e^2}{144 B_e^3} - \frac{\omega_e x_e}{4},$$

$$Y_{00}(\text{OH}) = 3.2 \text{ cm}^{-1}; Y_{00}(\text{OD}) = 2.5 \text{ cm}^{-1}; \quad (3)$$

and F_1 and F_2 are the ²Π rotational energies, as given by Hill and Van Vleck.¹² For the case of the vibrational ground state ($v'=0$) of an inverted ²Π_i state, and including the effect of centrifugal distortion term (we ignore the Λ doubling), we obtain

$$F_1^{\text{OH}}(J') = B_0^{\text{OH}} \{ (J' + 1/2)^2 - 1 - \frac{1}{2} [(2J' + 1)^2 + Y_0^{\text{OH}} (Y_0^{\text{OH}} - 4)]^{1/2} \} - D_0^{\text{OH}} (J' - 1/2)^2 \cdot (J' + 1/2)^2 \quad (4a)$$

and

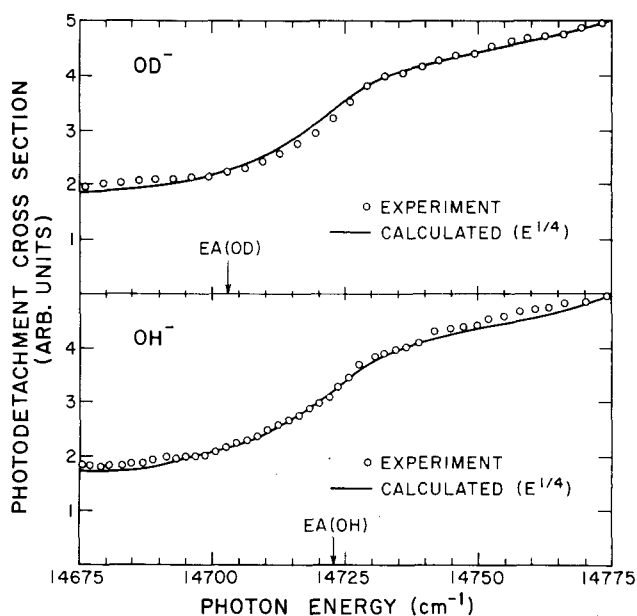


FIG. 2. OH⁻ and OD⁻ photodetachment cross sections in the energy range 14 675–14 775 cm⁻¹, containing the opening of the Q₃ rotational branch as defined in the text. The model photodetachment fits, as discussed in the text, were used in this energy range to determine E. A. (OH) and E. A. (OD). The OH⁻ and OD⁻ calculated cross sections (solid lines) were obtained with essentially the same assumed negative ion temperature and rotational line strengths. That the electron affinities of OH and OD appear at different places on the calculated curves is due to the different rotational energy level structure of OH and OD. The difference in the electron affinities can be ascribed almost entirely to differences in the position of the ground rotational state in OH(²Π_{3/2}) and OD(²Π_{3/2}). See text for more detail.

TABLE I. Molecular constants of OH, OD ($X^2\Pi$).^a

| | r_e (Å) | ω_e (cm ⁻¹) | $\omega_e x_e$ (cm ⁻¹) | B_0^b (cm ⁻¹) | A_0^b (cm ⁻¹) | Y_0 | $Y_0(Y_0 - 4)$ | D_0 (cm ⁻¹) |
|----|--------------|-----------------------------------|---------------------------------------|--------------------------------|--------------------------------|---------|----------------|------------------------------|
| OH | 0.9706 | 3735.2 ₁ | 82.8 ₁ | 18.515 | -139.7 | -7.547 | 87.15 | 18.65×10^{-4} |
| OD | 0.9699 | 2717.7 ₄ | 43.8 ₄ | 9.868 | -139.6 | -14.147 | 256.73 | 4.18×10^{-4} |

^aThese numbers are taken from Herzberg (Ref. 9).

^bThe values for B_0 and A_0 agree with those obtained by Herman and Hornbeck (Ref. 10) in a later study.

$$F_2^{\text{OH}}(J') = B_0^{\text{OH}} \{ (J' + 1/2)^2 - 1 + 1/2 [(2J' + 1)^2 + Y_0^{\text{OH}} (Y_0^{\text{OH}} - 4)]^{1/2} \} - D_0^{\text{OH}} (J' + 1/2)^2 \cdot (J' + 3/2)^2, \quad (4b)$$

where

$$Y_0^{\text{OH}} = A_0^{\text{OH}} / B_0^{\text{OH}}.$$

The rotational energy of the $v'' = 0$ state of OH⁻ is given by

$$F^{\text{OH}^-}(v'' = 0) = B_0^{\text{OH}^-} J''(J'' + 1) - D_0^{\text{OH}^-} J''^2 (J'' + 1)^2. \quad (4c)$$

Since it has been shown that $r_e(\text{OH}^-) = r_e(\text{OH})$ to within 0.1%⁸ and that the two potential curves are very similar in shape^{6,7} (near the bottom of the well at least) we can assume that

$$B_0^{\text{OH}^-} = B_0^{\text{OH}}, \quad (5a)$$

$$D_0^{\text{OH}^-} = D_0^{\text{OH}}. \quad (5b)$$

Possible errors introduced by these assumptions will be discussed later.

The connection of the term values with the electron affinity, which is the energy difference between the lowest state in OH($X^2\Pi_{3/2}$, $v' = 0$, $J' = 3/2$) and the lowest state in OH⁻($X^1\Sigma^+$, $v'' = 0$, $J'' = 0$) is (see Fig. 3)

$$\text{E. A. (OH)} = T_e^{\text{OH}} + E_0^{\text{OH}} + F_1^{\text{OH}}(3/2) - E_0^{\text{OH}^-}. \quad (6)$$

The formulas given above for OH and OH⁻ hold, of course, for OD and OD⁻, if the appropriate changes in the molecular constants are made (Table I). If the Born-Oppenheimer approximation is valid, one has $T_e^{\text{OH}} = T_e^{\text{OD}}$, i. e., there would be no electronic isotope shift. Such shifts have been observed, however, for hydrides and can have magnitudes of about 20 cm⁻¹ (for example, between the ground and first excited state in CuH and CuD).^{9,11} This shift has been discussed in detail by Bunker,¹¹ who was able to explain the major observations within the adiabatic approximation, which takes the diagonal corrections for the motion of the nuclei into account but does not, as in the Born-Oppenheimer approximation, assume fixed nuclei of infinite mass.

Besides the possibility of an electronic isotope shift, which is expected to be small ($\lesssim 20$ cm⁻¹), the electron affinities of OH and OD can be different as a result of differences in the vibrational zero-point energies for the neutral and negative ions, since

$$\begin{aligned} \text{E. A. (OH)} - \text{E. A. (OD)} &= T_e^{\text{OH}} - T_e^{\text{OD}} + E_0^{\text{OH}} - E_0^{\text{OH}^-} \\ &\quad - (E_0^{\text{OD}} - E_0^{\text{OD}^-}) \\ &\quad + F_1^{\text{OH}}(3/2) - F_1^{\text{OD}}(3/2). \quad (7) \end{aligned}$$

Furthermore, as follows from an inspection of the rota-

tional energies, one has for the present case

$$F_1^{\text{OH}}(3/2) - F_1^{\text{OD}}(3/2) = 13.3 \text{ cm}^{-1} \quad (8)$$

which means that even if there is no electronic isotope shift and if the vibrational zero-point energies cancel out exactly in Eq. (7) one has different electron affinities for OH and OD, E. A. (OH) being larger than E. A. (OD) by almost 2 meV (1 eV $\hat{=}$ 8065.466 cm⁻¹).¹³

B. Initial state distribution and rotational branches in the photodetachment process

The observed photodetachment cross section is composed of a large number of individual transitions from the various populated levels in the negative ion to the

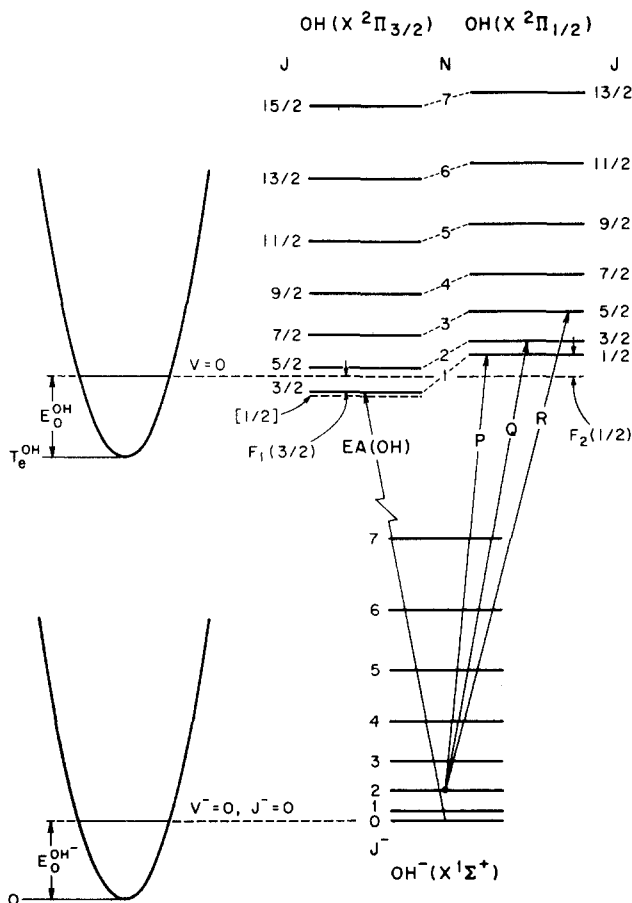


FIG. 3. Schematic energy level diagram for OH⁻($X^1\Sigma^+$) and OH($X^2\Pi_i$) showing what is meant by P, Q, and R rotational branches, and a representation of the various levels used in Eqs. (1)–(8) in the text. A similar diagram applies, of course, to OD.

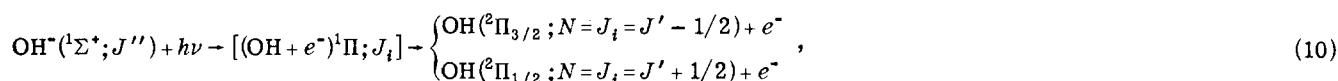
final rotational states in the neutral molecule. We will only consider transitions between the two vibrational ground states (0, 0). The justification for this is the fact that the vibrational spacing of about 3600 cm⁻¹ in the OH⁻ negative ion (which is essentially the same as in the OH neutral molecule; see also below) is about 3–4 times larger than the thermal energy kT of our ion source (estimate: 800 °K < T < 1800 °K; $kT = 1000$ cm⁻¹ for $T = 1440$ °K); one therefore expects that the $v'' = 1$ vibrational level in OH⁻ has only about 1%–5% of the population of $v'' = 0$. For OD⁻ the corresponding number is, of course, higher, namely 2%–12%. But even here we believe that neglecting (1, 1) transitions, which would appear in the same energy range as the (0, 0) transitions, does not affect our analysis, at least as far as the evaluation of the electron affinity is concerned. For the rela-

tive population of rotational states in the negative ion beam, we assume a Boltzmann distribution.

$$N(J'') = (2J'' + 1) \exp(-B_0'' J''(J'' + 1)/kT), \quad (9)$$

where the temperature T is a parameter in the fitting procedure. We are aware that the actual distribution may be different in shape as a result of nonequilibrium effects, particularly in the extraction region of the ion source; however, we cannot offer a more realistic approximation, and the fits to determine E. A. (OH) are not very sensitive to the choice of T , within the above range.

As a model for the photodetachment process near threshold we consider—similar to the discussion^{1,3,14} given for the photodetachment of S⁻ and Se⁻—the sequence



where J_i is the total angular momentum of the intermediate state “molecule + threshold electron” which has to be projected onto the actual final states¹⁵; the departing electron, which originates from a π orbital, is in an s wave. The assumption $J_i = N$ within this model is, of course, an approximation; it was chosen for the following reason: for most of the rotational levels of OH the system is closer to Hund’s case b than to Hund’s case a (the latter being a better description only for the very lowest rotational levels). In Hund’s case b the electron spin is coupled to N , which is close to being a “good” quantum number. The threshold electron (s wave) is loosely coupled to the molecule and not believed to project the intermediate state to final channels with $N \neq J_i$, but just to produce the two final states with spin up and down, $J' = J_i \pm 1/2$.

Given this model, we can attach some significance to the appearance of three rotational branches, which we shall call P, Q, R with the usual definition:

$$\begin{aligned} P: J_i &= J'' - 1, \\ Q: J_i &= J'', \\ R: J_i &= J'' + 1, \end{aligned} \quad (11)$$

so that we have to consider a total of six rotational branches, since there are two final electronic states, $^2\Pi_{3/2}$ and $^2\Pi_{1/2}$.

In detail we have

$$\begin{aligned} P3: \text{OH}^-(J'') \rightarrow \text{OH}(^2\Pi_{3/2}; J'' - 1/2) \quad J'' \geq 2 \\ Q3: \text{OH}^-(J'') \rightarrow \text{OH}(^2\Pi_{3/2}; J'' + 1/2) \quad J'' \geq 1 \\ R3: \text{OH}^-(J'') \rightarrow \text{OH}(^2\Pi_{3/2}; J'' + 3/2) \quad J'' \geq 0 \\ P1: \text{OH}^-(J'') \rightarrow \text{OH}(^2\Pi_{1/2}; J'' - 3/2) \quad J'' \geq 2 \\ Q1: \text{OH}^-(J'') \rightarrow \text{OH}(^2\Pi_{1/2}; J'' - 1/2) \quad J'' \geq 1 \\ R1: \text{OH}^-(J'') \rightarrow \text{OH}(^2\Pi_{1/2}; J'' + 1/2) \quad J'' \geq 0. \end{aligned} \quad (12)$$

The 3 refers, of course, to transitions terminating on OH($^2\Pi_{3/2}$), and the 1 to those terminating on $^2\Pi_{1/2}$.

These various transitions and their relationship to the electron affinity are shown pictorially in Fig. 3.

What can one say about the transition strength for the different rotational transitions? In the model, summarized in Eq. (10), one has to take the Hönl–London factors⁹ for the initial $^1\Pi - ^1\Sigma$ absorption process and then calculate the J_i dependence for the breakup of the intermediate state which involves the projection of the intermediate state onto the final states. We have not tried that; we simply assume here that the relative intensity of transitions within the same rotational branch is proportional to the relative population of the initial level $N(J'')$, as given in Eq. (9).

We further introduce weight factors W for the different branches, which allow for the possibility that the total intensity of different branches may be varied relative to each other. On the basis of the Hönl–London factors alone one would approximately have $W(R) \approx W(P) = 1/2$, $W(Q) = 1$. The J'' dependence for the intensity of the Q branch, as predicted by the Hönl–London factor, agrees, incidentally, with the one we adopt here.

C. Photodetachment threshold law for individual rotational onsets

Whereas the threshold law for photodetachment of atomic negative ions is well understood,^{1,3,4,16,17} little is known about the one for individual rotational transitions in the detachment of molecular negative ions, at least not for the case in which the final state molecule exhibits a permanent electric dipole moment [$\mu(\text{OH}) = 1.66$ D].¹⁸ Geltman¹⁹ has predicted the threshold behavior for molecular photodetachment in the case of short-range potentials. His analysis, which would predict $\sigma \propto E^{1/2}$ (σ : cross section; E : energy of detached electron) for OH⁻ detachment, does not apply in the present case, however. The influence of the long-range e^- -permanent dipole interaction ($\propto 1/r^2$) is expected to change the basic energy dependence¹⁶ which holds whenever long-range potentials (apart from the centrifugal

TABLE II. Positions of the thresholds for individual rotational transitions within the Q3 and Q1 branches in cm⁻¹ measured relative to the energy for the electron affinity transition OH⁻(J''=0) → OH(²Π_{3/2}, J' = 3/2).

| J' | OH | | OD | |
|------|-------------------------|-------------------------|-------------------------|-------------------------|
| | E _{thres} (Q3) | E _{thres} (Q1) | E _{thres} (Q3) | E _{thres} (Q1) |
| 1/2 | ... | 89.8 | ... | 111.8 |
| 3/2 | -37.0 | 77.0 | -19.7 | 103.8 |
| 5/2 | -27.2 | 67.2 | -12.8 | 96.8 |
| 7/2 | -19.8 | 59.7 | -6.9 | 90.9 |
| 9/2 | -14.1 | 54.0 | -1.8 | 85.9 |
| 11/2 | -9.7 | 49.6 | 2.4 | 81.6 |
| 13/2 | -6.2 | 46.1 | 6.1 | 77.9 |
| 15/2 | -3.4 | 43.3 | 9.2 | 74.8 |
| 17/2 | -1.1 | 41.4 | 11.9 | 72.1 |
| 19/2 | 0.8 | 39.1 | 14.2 | 69.8 |
| 21/2 | 2.4 | 37.5 | 16.3 | 67.7 |
| 23/2 | 3.7 | 36.2 | 18.0 | 66.0 |
| 25/2 | 4.9 | 35.0 | 19.6 | 64.4 |
| 31/2 | 7.6 | 32.3 | 23.3 | 60.7 |
| 41/2 | 10.5 | 29.5 | 27.4 | 56.6 |
| 51/2 | 12.3 | 27.7 | 30.1 | 53.9 |

potential) fall off more rapidly than $1/r^2$. In the presence of the electron-dipole potential $\mu P_1(\cos\theta)/r^2$, the leading term behavior of the cross section will lie between the two limiting cases $E^{1/2}$ and E^0 (step function), the exact shape of σ depending on the magnitude of the permanent dipole.¹⁷ O'Malley¹⁷ has treated the $e^- + H(n=2)$ final state (photodetachment of H⁻) as an example of an electron-dipole interaction. The difference between the permanent dipole case and the H($n=2$) case is that in the latter the "atomic dipole" is always directed towards the departing electron, so that the interaction energy does not contain the complicating angular dependence.

Branscomb⁶ has assumed step-function threshold behavior in his analysis of OH⁻, OD⁻ photodetachment. Steiner²⁰ concluded from his analysis of his SH⁻ and SD⁻ photodetachment data that $\sigma \propto (E^{1/2} + aE)$ gave the most satisfactory description.

It has to be stressed that one expects the threshold behavior to be a function of J' , since the effects of the rotation of the dipole field will be different for slow and fast rotation. The details of the interaction, as viewed for a single detachment process, depend on the direction in which the electron is ejected with respect to the molecular axis. In order to illustrate that the period of molecular rotation (T_{rot}) and the departure time of (T_{dep}) of the electron (we take the time an electron of energy E needs to travel 10 Å) are similar in the threshold region, we note that

$$T_{\text{rot}}(\text{OH}; J) \approx (9 \times 10^{-13} / J') \text{ sec}, \quad (13a)$$

$$T_{\text{dep}}(e^-, 10 \text{ \AA}, E) \approx [5 \times 10^{-14} / (E \text{ meV})^{1/2}] \text{ sec}, \quad (13b)$$

where E is the outgoing electron energy in millielectron volts. Under the present resolution the region of interest starts around 0.3–0.5 meV above threshold. For $E = 1$ meV, the rotation of the dipole will be sufficiently slow that it can be neglected only for the lowest J' val-

ues. In our analysis we have tried $\sigma \propto E^{1/2}$ and $\sigma \propto E^{1/4}$ for all J' in order to fit our data; step-function behavior could be excluded for significantly populated J states since we never had any indication for onsets that steep (even after convolution of a step with our bandwidth ≈ 2 cm⁻¹ $\hat{=}$ 0.25 meV).

D. Comparison of measurements with calculated cross section curves, determination of electron affinities

The calculation of a cross section curve involves the proper superposition of all possible rotational transitions. The threshold energies of these transitions can be calculated relative to the electron affinity. An estimate of the ion source temperature T can be obtained by an inspection of the P branch; we conclude that the range for T under our experimental conditions is $1000^\circ \text{K} \lesssim T \lesssim 1800^\circ \text{K}$, in good agreement with temperature estimates from S⁻ and Se⁻ detachment data.^{1,3} A comparison of the cross section in the range 14275–15415 cm⁻¹ with calculations based on either

$$\sigma \propto E^{1/2} \quad (14)$$

or

$$\sigma \propto E^{1/4} \quad (15)$$

for the energy dependence of the threshold OH⁻ photodetachment cross section shows much better agreement with the latter (average) threshold behavior of σ .

Theoretically one expects the threshold law to lie somewhere between the limiting cases $\sigma \propto E^0$ (step function) and $\sigma \propto E^{1/2}$ (no permanent dipole moment for OH), with the true threshold law being J dependent. By inspection of the quality of the fit over this broad energy range, where the details of branch strengths do not matter particularly, we conclude that $E^{1/2}$ is a too slowly rising function to describe the experimental data. Were the threshold law E^0 , we would have been able to discern distinct rotational onsets, which in fact we did not see. The $E^{1/4}$ law provided a much better qualitative fit over this broad energy range than either limiting case, and we have taken $E^{1/4}$ as the best "average" threshold law. One should not ascribe much significance to the exponent, however, except to note that it lies between 0 and 1/2.

The $E^{1/4}$ law also provided a distinctly better fit over more narrow energy ranges, such as is shown by the solid line in Fig. 1. The Q3 branch is fitted well, whereas the Q1 branch, as calculated, seems to be slightly shifted towards lower energies relative to the corresponding rise in the measured curve.²¹

The electron affinity is determined by detailed fits of the above photodetachment model to the experimental data in the energy region 14 675–14 775 cm⁻¹. The parameters which are allowed to vary are the negative ion rotational temperature, and the relative strengths of the P , Q , and R branches. Our fits to the OH⁻ and OD⁻ data near threshold are shown by solid lines in Fig. 2. In these fits we have chosen $T = 1200^\circ \text{K}$ together with the $E^{1/4}$ threshold law, and weights close to the Hönl-London weights. The photon energy corresponding to the electron affinity of OH (OD) is indicated by a vertical

line in Fig. 2. The fact that these two vertical lines occur at different places in the rising photodetachment cross section is a result of the different spacings and locations of energy levels in OH and OD. We see immediately from Fig. 2 that E. A. (OD) is less than E. A. (OH) by about 15–20 cm⁻¹.

Inspection of the dependence of the determination of E. A. on the different parameters leads to the following conclusions:

(a) the uncertainty in E. A. arising from the lack of precise knowledge of the negative ion beam internal state temperature is ± 5 cm⁻¹, at worst ± 10 cm⁻¹.²²

(b) the lack of knowledge of the weight factors W constitutes no problem, since we are extracting all the information about E. A. just from the steeply rising Q3 branch. The influence of a possible difference in transition strength from our assumption, as far as different transitions within the Q3 branch are concerned, has not been explored, since no good theoretical model was at hand to provide a possibly better description of the dependence of the transition strength on J'' than the one used by us. One may say that the uncertainties arising from this point are not greater than those mentioned in (a).

(c) The choice of the threshold law, which is purely empirical, is justified by the quality of the fit obtained; using the $E^{1/2}$ law Eq. (14), we were not able to get a satisfactory fit at all, unless unrealistic assumptions were made on the weights of different branches, and even then the agreement was not good.

(d) The uncertainty in the knowledge of B_0 and D_0 of the negative ion introduces minor errors; e.g., an uncertainty of B_0 of 0.1% gives an uncertainty of about ± 2 cm⁻¹ in E. A. (OH) and ± 1 cm⁻¹ in E. A. (OD). If $D_0(\text{OH}^-)$ agrees with $D_0(\text{OH})$ within 10%, the resulting uncertainty in E. A. (OH) is no more than 1 cm⁻¹; for OD, this error is negligible, since $D_0(\text{OD})$ is 4 times smaller than $D_0(\text{OH})$.

(e) In conclusion we obtain

$$\begin{aligned} \text{E. A. (OH)} &= (14723 \pm 15) \text{ cm}^{-1} \hat{=} (1.825_4 \pm 0.002) \text{ eV} \\ \text{E. A. (OD)} &= (14703 \pm 15) \text{ cm}^{-1} \hat{=} (1.823_0 \pm 0.002) \text{ eV} , \end{aligned} \quad (16)$$

where the numbers are the average over five single determinations of each E. A. by single fits, taking into account differences in negative ion beam temperature as inferred from differences observed for the P branches.

The difference in the electron affinities of OH and OD

$$\text{E. A. (OH)} - \text{E. A. (OD)} = 20 \text{ cm}^{-1}$$

we believe to be real and have a smaller uncertainty than one would conclude from the uncertainties in both separate E. A. values. The reason is that one expects systematic deviations as discussed in (a)–(d) to influence both E. A. 's in the same direction. We therefore think that ± 10 cm⁻¹ is a realistic error estimate on E. A. (OH) – E. A. (OD).

As discussed in IV. A, the isotope effect in E. A. expected from the different positions of the lowest level in OH and OD is 13.3 cm⁻¹ with the right sign, namely

E. A. (OH) > E. A. (OD). It therefore appears that most of observed differences in the E. A. 's can be explained that way.

This, in turn, means that the vibrational frequencies in the neutral and negative ions are very similar. Branscomb⁶ concluded that they agree (for OH) to within 560 cm⁻¹. From our data we can say, in the absence of an electronic isotope shift, that the difference in vibrational zero point energies is such as to produce a $(+7 \pm 10)$ cm⁻¹ difference in E. A. (OH) – E. A. (OD). This translates into the following bound for $\omega_e(\text{OH}^-)$ [Ref. 6, Eq. (12)]²³:

$$(+7 \pm 10) \text{ cm}^{-1} = 0.136 \{ \omega_e(\text{OH}) - \omega_e(\text{OH}^-) \}$$

or (17)

$$\omega_e(\text{OH}^-) = \omega_e(\text{OH}) - (51 \pm 74) \text{ cm}^{-1} .$$

If allowance is made for a possible electronic isotope shift one has to raise the uncertainties in Eq. (17) correspondingly. It should be noted that Cade obtained the result⁷

$$\omega_e(\text{OH}^-) > \omega_e(\text{OH}) \text{ by } 0 - 85 \text{ cm}^{-1} .$$

Since the dissociation energy of OH⁻ is about 0.36 eV larger than that of OH (the electron affinities of OH and O are different by that amount), and since the potential curves for OH⁻ and the ground state of OH are "well-behaved" (i.e., they have no "bumps" at larger internuclear distances), one might expect, indeed, that it is more likely that $\omega_e(\text{OH}^-) > \omega_e(\text{OH})$, as predicted by Cade.⁷ The error bar on our electron affinity difference E. A. (OH) – E. A. (OD) is unfortunately too large for definite conclusions in connection with this point. Thus we can summarize that, in agreement with Cade,⁷ the vibrational frequency in the OH⁻ negative ion is the same as that for OH within 50–100 cm⁻¹. The same conclusion holds for the pair OD–OD⁻.

ACKNOWLEDGMENTS

We are pleased to acknowledge very helpful correspondence with D. L. Albritton, P. R. Bunker, T. E. H. Walker, and R. N. Zare.

*This research was supported by the Advanced Research Projects Agency of the Department of Defense and was monitored by U. S. Army Research Office—Durham, under Contract No. DAHCO4 72 C 0047.

†On leave from Fakultät für Physik, Universität Freiburg, Freiburg Br, Germany; support by the Deutsche Forschungsgemeinschaft is gratefully acknowledged.

‡Alfred P. Sloan Foundation Fellow, 1972–1974.

¹W. C. Lineberger and B. W. Woodward, Phys. Rev. Lett. **25**, 424 (1970).

²W. C. Lineberger and T. A. Patterson, Chem. Phys. Lett. **13**, 40 (1972).

³H. Hotop, T. A. Patterson, and W. C. Lineberger, Phys. Rev. A **8**, 762 (1973).

⁴H. Hotop and W. C. Lineberger, J. Chem. Phys. **58**, 2379 (1973).

⁵S. J. Smith and L. M. Branscomb, Phys. Rev. **99**, A1657 (1955).

⁶L. M. Branscomb, Phys. Rev. **148**, 11 (1966).

⁷P. E. Cade, J. Chem. Phys. **47**, 2390 (1967).

- ⁸R. J. Celotta, R. A. Bennett, and J. L. Hall, *J. Chem. Phys.* (to be published).
- ⁹G. Herzberg, *Spectra of Diatomic Molecules, Vol. I, Molecular Spectra and Molecular Structure* (Van Nostrand, New York, 1950).
- ¹⁰R. C. Herman and G. A. Hornbeck, *Astrophys. J.* **118**, 214 (1953).
- ¹¹P. R. Bunker, *J. Mol. Spectrosc.* **28**, 422 (1968).
- ¹²E. Hill and J. H. van Vleck, *Phys. Rev.* **32**, 250 (1928).
- ¹³B. N. Taylor, W. H. Parker, and D. N. Langenberg, *Rev. Mod. Phys.* **41**, 375 (1969).
- ¹⁴A. R. P. Rau and U. Fano, *Phys. Rev. A* **4**, 1751 (1971).
- ¹⁵In fact one should not use the Hund's case a designations in Eq. (10), for the $^2\Pi_{1/2}$ and $^2\Pi_{3/2}$ states are really linear combinations of the two possible J_i final states of the separated complex. This notation is used to emphasize the fact that one should view the photodetachment process near threshold as the formation of a complex (electron + neutral) which then has to be projected onto the actual final states. For the precise linear combinations required in this projection see: G. C. Dousmanis, T. M. Sanders, Jr., and C. H. Townes, *Phys. Rev.* **100**, 1735 (1955).
- ¹⁶E. P. Wigner, *Phys. Rev.* **73**, 1002 (1948).
- ¹⁷T. F. O'Malley, *Phys. Rev.* **137**, A1668 (1965).
- ¹⁸F. X. Powell and D. R. Lide, *J. Chem. Phys.* **42**, 4201 (1964).
- ¹⁹S. Geltman, *Phys. Rev.* **112**, 176 (1958).
- ²⁰B. Steiner, *J. Chem. Phys.* **49**, 5097 (1968).
- ²¹It should be stressed that the Q3 and Q1 branches are by no means separated by an amount equal to the spin-orbit coupling constant (-139.7 cm^{-1}). This is clearly seen in Table II, which gives the onset energies for the various rotational transitions within the Q3 and Q1 branches with respect to the energy of the electron affinity. In this point Branscomb's analysis (Ref. 6) was incorrect since he assumed Q3 and Q1 to be apart by 139.7 cm^{-1} (taking Hund's case a for OH, which is far from being correct). The same criticism applies to Steiner's analysis of his SH⁻ and SD⁻ photodetachment (Ref. 20), through, of course, SH is much closer of Hund's case a than is OH.
- ²²This rather small dependence on T can be anticipated from the onset energies for the different rotational transitions within the Q3 branch (at least as long as the internal negative ion beam temperature is not too small).
- ²³Use of more complicated expressions than those employed by Branscomb (Ref. 6) does not seem to be justified here.